Synthesis and Analysis of Ag-Ag_2O/Supported TiO_2 for using as a Bactericide

Surangkana Wannapop [a,*] Aiya Chantarasiri [a], Parima Boontanom [a], Titipun Thongtem [b, d] Somchai Thongtem [c, d]

[a]*Faculty of Science, Energy and Environment, King Mongkut's University of Technology North Bangkok, Rayong Campus, Rayong, 21120 Thailand*
[b]*Department of Chemistry, Faculty of Science, Chiang Mai University, Chiang Mai, 50200 Thailand*
[c]*Department of Physics and Materials Science, Faculty of Science, Chiang Mai University, Chiang Mai, 50200 Thailand*
[d]*Materials Science Research Center, Faculty of Science, Chiang Mai University, Chiang Mai, 50200 Thailand*

Received 16 December 2017; Revised 13 March 2018; Accepted 28 March 2018

Abstract

TiO_2 and Ag-Ag_2O/supported TiO_2 nanoparticles were successfully synthesized by a cyclic-microwave method. The products were characterized by X-ray powder diffraction (XRD), scanning electron microscopy (SEM) and UV-visible spectroscopy, including the determination for antibacterial activity through the use of *S. aureus* and *E. coli* as a model. In this research, the mixed phases of bactericide exhibited excellent antibacterial activities: 100% for both *S. aureus* and *E. coli* by 0.005 – 1 w/v% of 0.8 mmol Ag-Ag_2O/supported TiO_2, except for 62.82% of *S. aureus* by 0.005 w/v% of the bactericide.

KEYWORDS: Ag-Ag_2O/supported TiO_2; XRD; SEM; Antibacterial activity

* Corresponding authors; e-mail: surangkana.w@sciee.kmutnb.ac.th

Introduction

TiO_2 is an n-type semiconductor with 3.2 eV energy gap [1] and can be excited by ultraviolet (UV) radiation which is available only 5% of the total solar radiation. Thus it is not practical to be used as a renewable energy material [2]. Efforts have been taken to extend the photonic response of this material ranging from UV to visible radiation by doping with metals, such as Si, Fe, Ag, Au and Pt [2 – 5]. Ag deposition on TiO_2 surface can enhance photo-oxidation of oxalic acid five times, due to the increasing in the content of excited oxygen [6]. Ag-Ag_2O/supported TiO_2 has a lot of applications: photocatalysis [4, 7, 8], water splitting [9], antibacterial activity [10 – 12] and dye-sensitized solar cells [13, 14].

In this research, cyclic microwave radiation was selected to synthesize TiO_2 and Ag-Ag_2O/supported TiO_2, due to many benefits such as very simple, fast, inexpensive and extremely effective. This procedure can solve the problem of concentration and temperature gradients. The TiO_2 and Ag-Ag_2O/supported TiO_2 nanomaterials were thoroughly characterized by several techniques to predict morphology and phase. Antibacterial activity of the semiconductor was evaluated through the use of *Escherichia coli* strain (Gram negative bacteria) and *Staphylococcus aureus* (Gram positive bacteria).

Materials and Methods

Titanium (IV) butoxide (purum ≥ 97%) and silver nitrate were used as Ti and Ag precursors. TiO_2 and Ag-Ag_2O/supported TiO_2 were prepared by controlled addition of 1 ml titanium precursor in 40 ml mixture containing 20 ml deionized water and 20 ml of 95% ethanol with constant stirring, including 0 – 3.2 mmol Ag of silver nitrate addition to each of the 40 ml mixture. Subsequently, 3.5 mmol cetyltrimethylammonium bromide (CTAB) was added to the solutions. To avoid over boil, the mixed solutions were cyclically irradiated by 450 W microwave with 60 s on for every 60 s interval for 15 min. The as-prepared precipitates were washed with deionized water and 95% ethanol, and dried at 80 ^oC for 12 h. The final products were calcined at 400 °C for 2 h for further characterization by XRD (Rigaku Miniflex Π) with a Cu-K_{α} line (λ = 0.1542 nm), SEM (JEOL JSM-6335F) operated at 15.0 kV and a UV-visible spectrometer (SHIMADZU UV 2006) using a UV lamp with the resolution of 1 nm.

Antibacterial activity of the nanoparticles was evaluated through two bacterial species: *Escherichia coli* strain (Gram negative bacteria) and *Staphylococcus aureus* (Gram positive bacteria). The first was provided by the Thailand Institute of Scientific and Technological Research, Thailand, and the second by the Department of Microbiology, Faculty of Science, Mahidol University. Bacteria were growth in the Tryptone Soya Broth (HiMedia, India) at 37 °C for 16 h under agitation condition to obtain an optical density at 600 nm of 0.6. Bacterial suspension was prepared and adjusted to obtain 10^{-3} dilution by serial diluting with the sterile Tryptone Soya Broth. TiO_2 and Ag-Ag_2O/supported TiO_2 nanoparticles were suspended in bacterial suspension at the final concentration of 1 – 0.005 w/v% and incubated at a temperature of 37 °C for 30 min in the dark condition. 100 µl of bacterial suspension was spread on the Tryptone Soya Agar (HiMedia, India). Positive control was studied by spreading bacterial suspension without nanoparticles on the Tryptone Soya Agar. All agar plates were incubated at 37 °C for 16 h in the dark condition and evaluated for the number of viable bacterial colonies.

Results and Discussion

XRD patterns (Fig. 1) of TiO_2 and Ag-Ag_2O/supported TiO_2 with different Ag contents show the peaks at 2θ of the 25.306°, 37.779°, 48.039°, 53.859°, 55.058° and which were indexed to the (101), (004), (200), (105), and (2 1 1) planes of anatase TiO_2 (JCPDS database no. 21-1272) [15]. A peak at 2θ of 25.737° was also detected and indexed to the (210) plane of brookite TiO_2 (JCPDS database no. 75-1582) [15]. The positions of major diffraction peaks of the Ag-Ag_2O/supported TiO_2 samples were similar to those of the unsupported TiO_2, except for the change in their intensities. Upon supporting with 0.8 – 3.2 mmol Ag, additional peaks at 2θ of 31.117° and 54.711° were detected and attributed to the (111) and (220) crystalline planes of silver (I) oxide (Ag_2O) with cubic structure (JCPDS database no. 12-0793) [15]. Additional peaks at 2θ of 44.335° and 64.678° were detected and attributed to the (200) and (220) crystalline planes of silver with cubic structure (JCPDS database no. 04-0783) [15]. The intensities of Ag_2O and Ag peaks increase with the Ag content increasing. The particle sizes of anatase, Ag_2O and Ag nanoparticles were determined by Scherrer formula [7], as the results summarized in Table 1. Crystallite sizes of anatase, Ag_2O and Ag nanoparticles were increased with the increasing the Ag content.

In this research, the 0.8 mmol Ag-Ag_2O/supported TiO_2 product contained the smallest nanoparticles. For 1.6 – 3.2 mmol Ag-Ag_2O/supported TiO_2, the anatase and Ag crystallites were smaller than the Ag_2O one. The reverse is true for 0.8 mmol Ag-Ag_2O/supported TiO_2 product. The results showed that the Ag_2O crystallite grew very rapidly, accelerated by Ag loading material.

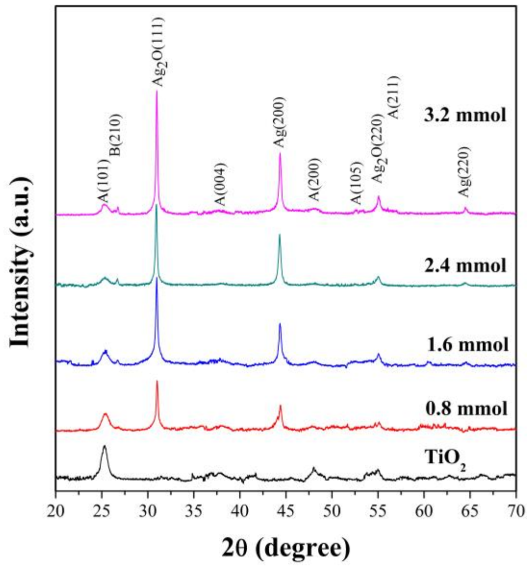

Fig. 1 XRD patterns of TiO_2 and 0.8 – 3.2 mmol Ag-supported TiO_2.

Table 1 Crystallite sizes of the anatase, Ag and Ag_2O products.

Products	Crystallite sizes of TiO_2 and Ag-supported TiO_2 samples (nm)				
	TiO_2	0.8 mmol	1.6 mmol	2.4 mmol	3.2 mmol
Anatase (101)	15.776	21.997	42.070	55.077	63.111
Ag (200)	-	15.992	22.851	26.655	26.683
Ag_2O (111)	-	11.106	76.786	86.825	86.929

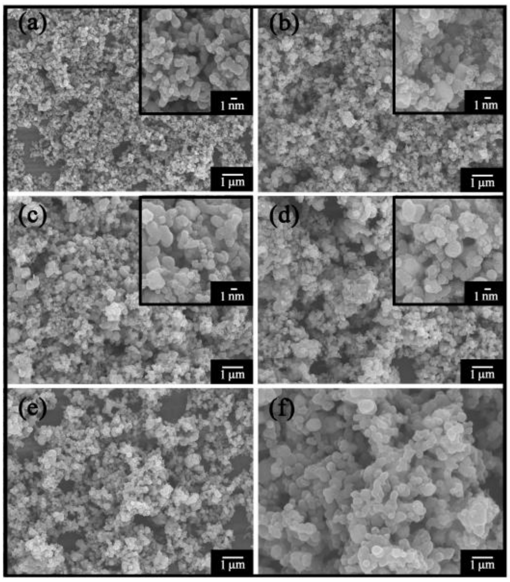

Fig. 2 SEM images of (a) TiO_2, (b) 0.8 mmol Ag-Ag_2O/supported TiO_2, (c) 1.6 mmol Ag-Ag_2O/ supported TiO_2, (d) 2.4 mmol Ag-Ag_2O/supported TiO_2 and (e – f) 3.2 mmol Ag-Ag_2O/supported TiO_2.

In general, TiO_2 and Ag-Ag_2O/supported TiO_2 (Figure 2) were composed of a number of uniform nanoparticles oriented in all directions. The more content of Ag was supported, the larger particles were detected. Among the Ag-Ag_2O/supported TiO_2 samples, 0.8 mmol Ag-Ag_2O/ supported TiO_2 sample was the smallest (largest surface area) and was used for antibacterial testing. All 0.005 – 1 w/v% of 0.8 mmol Ag-Ag_2O/supported TiO_2 samples were tested for antibacterial activities for both *E. coli* (gram-negative) and *S. aureus* (gram-positive), as the results shown in Figures 3 & 4 and Table 2. In this research, all bacteria were totally killed, except for the test by using 0.005 w/v % bactericide for *S. aureus*. The higher Ag content and the zone can finally reach the 100 % bacteria killing in the dark without the need of light irradiation, except for the test for *S. aureus* by 0.005 w/v% bactericide. Possibly, a lot of Ag nanoparticles containing in TiO_2 can lead to another environmental risk, caused by the removal of Ag nanoparticles from host material – due to chemical equilibrium. Mostly oxidation states of silver are Ag^0 and Ag^+. They can combine with anions such as sulfide, bicarbonate, sulfate and chloride. Thus, antibacterial activities of Ag-Ag_2O/supported TiO_2 will be reduced when the environment contains these anions. The 0.8 mmol Ag-Ag_2O/supported TiO_2 with 0.005 – 1 w/v% concentrations was used as a bactericide. For the concentration of 0.005 w/v%, *S. aureus* with thick wall of peptidoglycan was killed for 62.82% and *E. coli* with thin wall of lipopolysaccharide was totally killed [16], comparing with the corresponding controls.

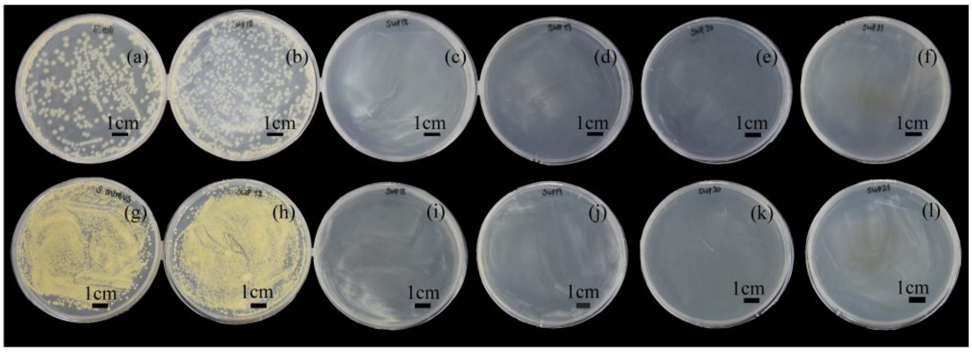

Fig. 3 Antibacterial activities for (a–f) E. coli and (g–l) *S. aureus* by controls, TiO_2, 0.8, 1.6, 2.4 and 3.2 mmol Ag-Ag_2O/supported TiO_2, respectively.

Table 2 Antibacterial activities (%) of 0.8 mmol Ag-Ag_2O/supported TiO_2 with different concentrations.

Bacteria	Concentration of bactericide (w/v%)									
	1	0.8	0.6	0.4	0.2	0.1	0.05	0.025	0.01	0.005
E. coli	100	100	100	100	100	100	100	100	100	100
S. aureus	100	100	100	100	100	100	100	100	100	62.82

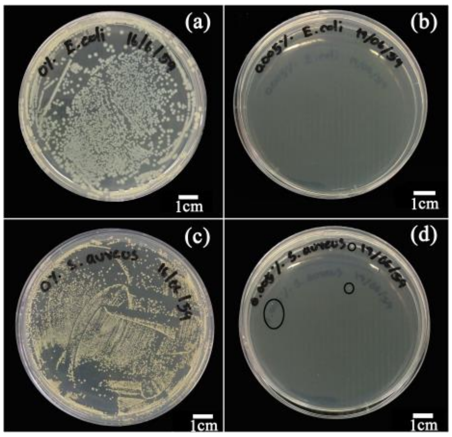

Fig. 4 Antibacterial activities of (a, c) controls and (b, d) after treat 0.005 w/v% of 0.8 mmol Ag-Ag_2O/supported TiO_2 for *E. coli* and *S. aureus*, respectively.

UV–visible absorption of TiO_2 and the Ag-Ag_2O/supported TiO_2 samples are shown in Figure 5. These spectral features can be attributed to the plasmon resonance absorption, which shows that Ag nanoparticles give rise to a band in the visible range with longer wavelengths with increase in the metal loading, excluding those of the 3.2 mmol Ag-Ag_2O/supported TiO_2 sample, caused by the highest concentration and the largest crystallite size of silver and silver (I) oxide nanoparticles.

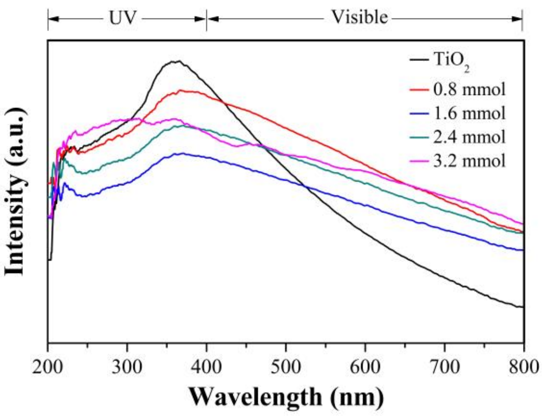

Fig. 5 UV–visible absorption of TiO_2, 0.8, 1.6, 2.4 and 3.2 mmol Ag-Ag_2O/supported TiO_2 samples

Conclusion

In this research, silver- silver (I) oxide-anatase-brookite mixed phases were successfully synthesized by a cyclic microwave method. The desired properties were modified to be used as a bactericide with very high efficiency against both gram-negative and gram-positive bacteria. Upon supporting with 0.8 mmol of Ag loading material, antibacterial efficiency was detected: 100 % killing for both *E. coli* and *S. aureus* by 0.005 – 1 w/v% bactericide, except for 62.82% killing of *S. aureus* by 0.005 w/v% bactericide.

Acknowledgements

This research was funded by King Mongkut’s University of Technology North Bangkok. Contract no. KMUTNB-NEW-58-20.

References

[1] J.V. Hernandez, S. Coste, A.G. Murillo, F.C. Romo, A. Kassiba, Effects of metal doping (Cu, Ag, Eu) on the electronic and optical behavior of nanostructured TiO_2, J. Alloy Compd. 710 (2017) 355 – 363.

[2] S. Chen, B. Lv, Yao Xu, Fe-quinoline complexes sensitized Si-doped TiO_2 with enhanced visible light photocatalytic activity, Mater. Lett. 77 (2012) 32 – 34.

[3] S. Demirci, T. Dikici, M. Yurddaskal, S. Gultekin, M. Toparli, E. Celik, Synthesis and characterization of Ag doped TiO_2 heterojunction films and their photocatalytic performances, Appl. Surf. Sci. 390 (2016) 591 – 601.

[4] Y. Cui, Q. Ma, X. Deng, Q. Meng, X. Cheng, M. Xie, X. Li, Q. Cheng, H. Liu, Catalytic performance of the Pt/TiO_2 catalysts in reverse water gas shift reaction: Controlled product selectivity and a mechanism study, Appl. Catal. B. 206 (2017) 136 – 145.

[5] E. Albiter, M.A. Valenzuela, S. Alfaro, G. Valverde-Aguilar, F.M. Martı´nez-Pallares, Photocatalytic deposition of Ag nanoparticles on TiO_2: Metal precursor effect on the structural and photoactivity properties, J. Saudi Chem. Soc. 19 (2015) 563 – 573.

[6] H.T. Ren, Q. Yang, Fabrication of Ag_2O/TiO_2 with enhanced photocatalytic performances for dye pollutants degradation by a pH-induced method, Appl. Surf. Sci. 396 (2017) 530 – 538.

[7] T. sun, E. liu, J. Fan, X. Hu, F. Wu, W. Hou, Y. Yang, L. Kang, High photocatalytic activity of hydrogen production from water over Fe doped and Ag deposited anatase TiO_2 catalyst synthesized by solvothermal method, Chem. Eng. J. 288 (2013) 896 – 906.

[8]Y. Li, M. Ma, W. Chen, L. Li, M. Zen, Preparation of Ag-doped TiO_2 nanoparticles by a miniemulsion method and their photoactivity in visible light illuminations, Mater. Chem. Phys. 129 (2011) 501 – 505.

[9] J.V. Hernandez, S. Coste, A.G. Murillo, F.C. Romo, A. Kassiba, Effects of metal doping (Cu, Ag, Eu) on the electronic and optical behavior of nanostructured TiO_2, J. Alloy Compd. 710 (2017) 355 – 363.

[10] L. Gao, W. Gan, S. Xiao, X. Zhan, J. Li, A robust superhydrophobic antibacterial Ag-TiO_2 composite film immobilized on wood substrate for photodegradation of phenol under visible-light illumination, Ceram. Intl. 42 (2016) 2170 – 2179.

[11]X. Zhang, M. Li, X. He, R. Hang, X. Huang, Y. Wang, X. Yao, B. Tang, Antibacterial activity of single crystalline silver-doped anatase TiO_2 nanowire arrays, Appl. Surf. Sci. 372 (2016) 139 – 144.

[12] X. Hou, H. Ma, F. Liu, J. Deng, Y. Ai, X. Zhao, D. Mao, D. Li and B. Liao, Synthesis of Ag ion-implanted TiO_2 thin films for antibacterial application and photocatalytic performance, J. Hazard. Mater. 299 (2015) 59 – 66.

[13] K. Usha, P. Kumbhakar, B. Mondal, Effect of Ag-doped TiO_2 thin film passive layers on the performance of photo-anodes for dye-sensitized solar cells, Mater. Sci. Semicond. Proc. 43 (2016) 17 – 24.

[14] H. Hu, J. Shen, X. Cao, H. Wang, H. Lv, Y. Zhang, W. Zhu, J. Zhao, C. Cui, Photo-assisted deposition of Ag nanoparticles on branched TiO_2 nanorod arrays for dye-sensitized solar cells with enhanced efficiency, J. Alloy Compd. 694 (2017) 653 – 661.

[15] Powder Diffract. File, JCPDS-ICDD, 12 Campus Bld., Newtown Square, PA 19073-3273, U.S.A., 2001.

[16] N. Ekthammathat, T. Thongtem, S. Thongtem, Antimicrobial activities of CuO films deposited on Cu foils by solution chemistry, Appl. Surf. Sci. 277 (2013) 211 – 217.